Abburi Venkata, K., Truman, C., Coules, H., Dey, S., & Pirling, T. (2017). Assessment of the effect of residual stresses in elastic-plastic fracture of dissimilar welded components. *Materials at High Temperatures*, *34*(5-6), 492-499. https://doi.org/10.1080/09603409.2017.1378965

Assessment of the effect of residual stresses in elastic-plastic fracture of dissimilar welded components

K. Abburi Venkata[a]*, S. Dey[a], H.E. Coules[a], C.E. Truman[a] and T. Pirling[b]

[a]*Department of Mechanical Engineering, University of Bristol, Bristol, UK;*

[b]*Institut Laue-Langevin, Grenoble, France*

*corresponding author: Dr K. Abburi Venkata, Postdoctoral Research Associate, 1.25 Queen's Building, University of Bristol, University Walk, Bristol, BS8 1TR, UK

Email address: k.abburivenkata@bristol.ac.uk

Assessment of the effect of residual stresses in elastic-plastic fracture of dissimilar welded components

Residual stresses in welds pose a significant threat to the structural integrity of a component, especially in the presence of defects and are required to be accounted for in assessing component safety. Although the R6 assessment procedure suggests various approximate methods for incorporating these effects in defect assessment, most of them are overly conservative and not very cost-effective. A more reliable approach is to characterise the weld residual stresses around a defect and study how they interact with primary load. The current paper analyses the effects of weld residual stresses on the fracture of a dissimilar weld in the presence of defect. The weld is made between modified 9Cr-1Mo steel and 316LN stainless steel using autogenous electron beam welding. A C(T) specimen was extracted from the centre of the weld and a crack introduced in the fusion zone using electro-discharge machining (EDM).

The residual stresses around the crack were measured on a grid of measurement points at mid-thickness of the C(T) specimen using neutron diffraction on the strain diffractometer SALSA at ILL, Grenoble. The measured residual stresses around the crack-tip were incorporated into a finite element (FE) model and the interaction of these with applied load was predicted under fracture.

Keywords: Weld residual stresses; elastic-plastic fracture; neutron diffraction; finite element analysis

Introduction

Dissimilar welds are often used in nuclear power plants to join one component to another and usually operate under high temperature and pressure environments. As welding is a source of very large residual stresses, localised as well as long-range, and result in plastically deforming the material, it is generally required to study these joints thoroughly in order to understand the influence and effects of these on structural integrity and how

they contribute to failure in service. In general, residual stresses contribute to crack driving forces and have a strong influence on the fracture toughness of the material [1 - 3]. The combined primary and secondary loading might promote the propensity to fracture or change the mode of failure based on the extent of plasticity in a component [1, 2]. Added to this is the complexity arising from relaxation of residual stresses during service which will affect the crack-tip constraint and thereby change the fracture behaviour.

For linear elastic fracture mechanics (LEFM) considerations, the effect of residual stresses on fracture can be obtained by calculating the total stress intensity factor (K) by superposition of residual stresses with mechanical loading [2]. This is valid as long as the material response is elastic. However, in situations with plastic deformation, the linearity is no longer valid and the elastic-plastic fracture parameter J cannot be determined by simply superposing residual stresses with applied loading and requires defect assessment procedures outlined in R6, BS 7910 [4, 5] or finite element (FE) simulation to accurately model the effect of residual stresses/strains on crack propagation and elastic-plastic fracture [6, 7].

In the current paper, the residual stresses ahead of a crack-tip in a dissimilar weld are predicted using FE analysis. For this purpose, first the welding process was simulated using ABAQUS code v6.14 and the welding residual stresses/strains were predicted in the weld plate [8, 9]. In the second stage, a C(T) specimen was extracted from the welded plate using EDM process. This is simulated again using ABAQUS by providing the residual stresses predicted in the welded plate as initial condition and the relaxation from the machining process was predicted [10].

In the third stage, an EDM notch is introduced into the C(T) blank specimen, followed by a fatigue pre-cracking to create a sharp crack in the centre of the weld fusion

zone. The crack extended through the thickness of the specimen. The residual stresses around the sharp crack in the form of a grid were measured using neutron diffraction on strain diffractometer SALSA at ILL Grenoble, France. Also, the FE model was extended to simulate introduction of sharp crack in the C(T) blank specimen, in the presence of residual stresses. The residual stresses around the crack-tip were predicted and compared against those from measurements. The C(T) crack model thus validated was used to predict the modified J integral under combined loading from applied and residual stresses. The details of the first two stages were published elsewhere [8 - 10]. The details of the fatigue pre-cracking, neutron diffraction experiment and the FE analysis are presented below and the results discussed.

Sample and experimental details

The sample is a C(T) specimen extracted from a dissimilar weld between ferritic-martensitic 9Cr-1Mo (P91) steel and austenitic 316LN stainless steel using electron beam (EB) welding. The welding was performed by applying first a full penetration pass followed by a cosmetic pass with ~ 4.5 mm depth of penetration. The weld fusion zone width is ~ 1.1 mm in the weld pass and ~ 3.5 mm in the cosmetic pass. The heat affected zone is ~ 0.7 mm in width. The chemical composition of the parent materials, the elastic properties and the monotonic stress-strain response are provided elsewhere [11]. The schematic of the C(T) specimen and the cross-sectional weld macrograph are shown in Fig. 1. In the C(T) specimen an EDM notch is machined for a length of 2 mm using 0.2 mm wire. The notch is introduced along the weld centreline throughout the thickness of the specimen.

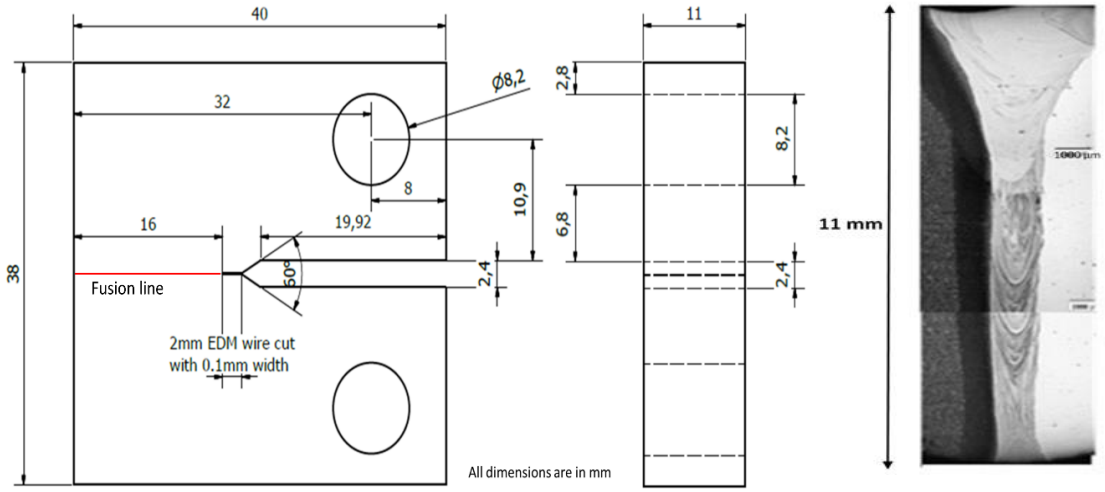

Fig. 1. Schematic of (left) C(T) specimen (Right) cross-sectional weld macrograph

Fatigue pre-cracking

Subsequent to EDM notch creation, the specimen is fatigue pre-cracked on a tensile testing machine to introduce a sharp crack at the tip of EDM notch. The mean load for fatigue pre-cracking was derived based on the recommendations from ASTM standard (E1820-15a) [12] for C(T) specimen as a mean load of 2 kN with an amplitude of 1.6 kN. This was applied until a pre-crack of sufficient length (~ 0.8 mm) was generated. The optical images of the pre-crack are shown in Fig. 2.

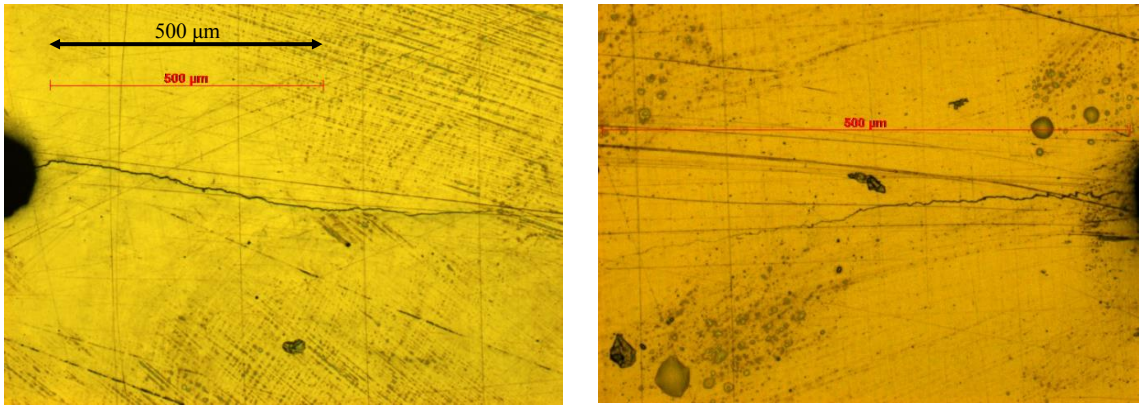

Fig. 2. Fatigue pre-cracking on the specimen's front face (left) and back face (right).

Neutron diffraction

In order to measure the residual stress/strain field around the crack-tip, neutron diffraction was conducted on the SALSA strain diffractometer at the ILL facility in Grenoble, France. The stresses/strains were measured on a grid of 9 x 9 points around the crack-tip at mid-thickness of the specimen. The schematic of the measurement grid is shown in Fig. 3. In order to capture the steep gradients of stress across the weld, the grid spacing was set to 0.5 mm.

As SALSA uses a monochromatic source of neutrons, the diffraction pattern was based on reflections from a single set of crystallographic planes and were chosen as <211> for the bcc phase and <311> for the fcc phase. These planes were chosen as they are relatively insensitive to any intergranular stresses as well as the elastic constants on these planes closely correspond to that of the bulk material [13, 14]. The first line on the grid was 0.5 mm away from the EDM notch. A gauge volume of 0.6 mm x 1 mm x 0.6 mm was employed for measuring longitudinal strain (parallel to the weld) because of the steep gradients in stress across the weld, characteristic of this welding process and later extended to 0.6 mm x 2 mm x 0.6 mm for measurements in the transverse and normal directions. The d0 measurements were made at mid-thickness of the specimen at exactly the same locations corresponding to those on the C(T) specimen, across the weld.

The data from the experiment was analysed using the software *LAMP* to determine the lattice spacing. The peak fitting was performed using reflections from a single set of crystallographic planes as explained above. The strain was calculated using the relation [13],

$$\varepsilon_{xx} = \frac{d_x - d_{ox}}{d_{ox}} \quad (1)$$

where d_x, d_{ox} are the lattice spacing measured in C(T) specimen and reference specimen respectively and ε_{xx} is the elastic strain along x-direction. The calculated strain was further used to determine the stress using [13]

$$\sigma_{xx} = \frac{E}{(1-\nu)}[\varepsilon_{xx} + \frac{\nu}{(1-2\nu)}(\varepsilon_{xx} + \varepsilon_{yy} + \varepsilon_{zz})] \quad (2)$$

where σ_{xx} is the stress along x-direction. E and ν are the Young's modulus and Poisson's ratio respectively. The values of E and ν were assumed as 210 GPa and 0.3 for P91 steel and 195.6 GPa and 0.294 for 316LN steel respectively based on the recommendations from Kröner's model for the macroscopic elastic bulk properties in poly-crystals for bcc and fcc phases [13].

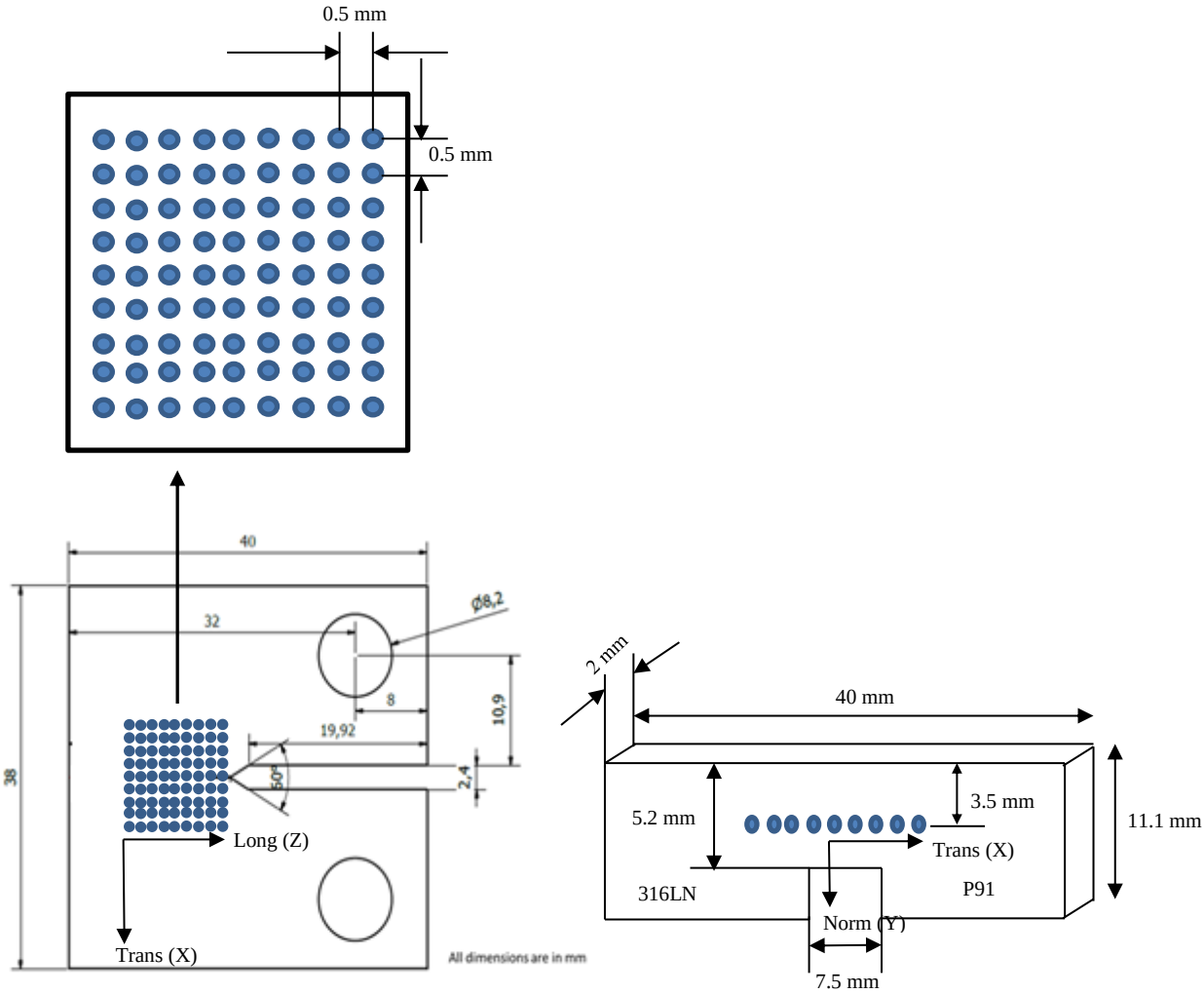

Fig. 3. Schematic of the measurement grid on the C(T) specimen (left) and the d0 specimen (right).

Finite element analysis

In order to investigate the effect of residual stresses on fracture, FE analysis is conducted using ABAQUS 6.14 code to predict mode I stress-intensity factor for crack-tip loading under residual stresses. The residual stresses retained in the C(T) specimen from the welding process were determined using two different approaches. In the first approach, the entire welding process is simulated using sequentially coupled thermo-mechanical analysis and the residual stresses were predicted in the welded plate. Later the C(T) blank specimen extraction is modelled using element deactivation to predict the residual stress relaxation during the machining processes. In the second approach, the residual stresses measured on the C(T) blank specimen using neutron diffraction on the E3 strain diffractometer at the HZB facility were mapped into the FE model using the predefined field and the stresses were allowed to equilibrate over the specimen dimensions [10].

The residual stress profiles were compared from both the approaches and used as a validation for the residual stresses predicted from the FE weld analysis. Based on the mapping of measured residual stresses on the C(T) blank specimen and the material hardening data (equivalent plastic strain) predicted from the weld model, the initial condition to the C(T) specimen prior to the introduction of the crack is supplied. Any plasticity accumulated during the welding process, is removed from further crack analysis models. This is done to avoid accounting prior plasticity in the mechanical strain energy release rate during modified J-integral evaluation, but ensuring that the initial strains are considered in the evaluation of J-integral [15]. The propagation of the crack is modelled instantaneously for the combined length of the EDM notch and fatigue pre-crack (3 mm). The modified J-integral values for various loading cases are predicted around the crack-tip.

In addition to modified J-integral predictions, linear elastic fracture mechanics (LEFM) analyses were conducted to predict the mode I stress-intensity factor K_I in the

presence of residual stresses. The predicted K_I is compared with that determined using the analytical weight function method and the residual stresses measured in the C(T) blank specimen. The weight function method was based on the stress-intensity factor solutions provided by Wu and Carlson [16] for the C(T) geometry. The various results are presented and discussed in next section.

Results and Discussion

Measured residual stress profiles around crack-tip from ND

The measured longitudinal residual stress profile around the crack-tip on the SALSA strain diffractometer is shown in Fig. 4 as a contour map. The crack-tip is shown with a bold black edge. The distance y is across the weld and x is along the weld. It can be observed that there is significant stress around the crack-tip and that the crack-tip is under compressive loading. This is because of the compressive residual stress state observed in the weld centre due to solid-state phase transformation experienced during the welding process.

However, it is evident from the tensile peaks adjacent to the weld fusion zone that there is a steep gradient in stress over a very small length scale (~0.5 mm). Considering such a residual stress distribution in the evaluation of the material fracture behaviour is quite cumbersome. For instance, for the given crack location, the compressive residual stresses around the crack-tip might hinder the crack advancement.

Nevertheless, if the crack location is shifted slightly on either side of the weld by a small amount (~ 0.5 mm) would result in significantly different results. A prudent thing in such evaluation would be to completely ignore the compressive stresses in the weld centre and assume a peak tensile stress throughout the weld fusion zone and HAZ and calculate the fracture parameters accordingly, although the accuracy of such results is debatable. Added to this there is the further complication of smaller gauge volume

employed during the measurement, resulting in the second order residual stresses such as phase dependent residual stresses not being in equilibrium and thereby affecting the

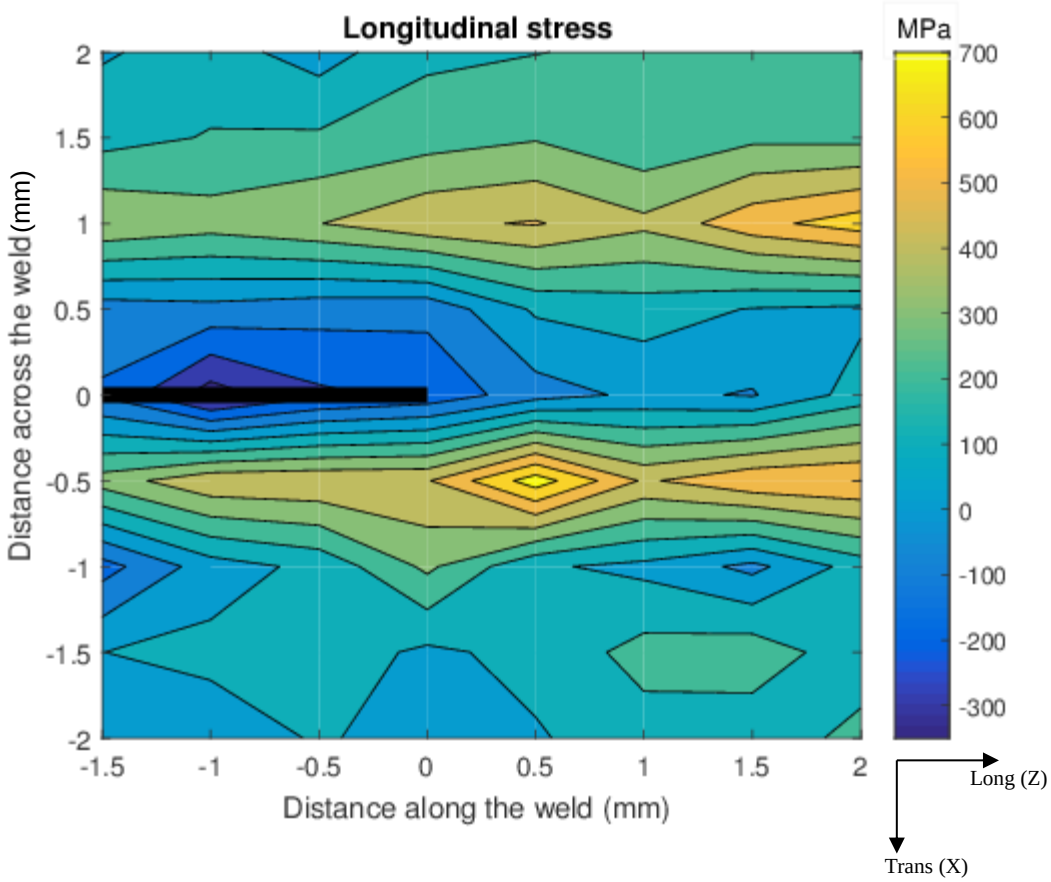

Fig. 4. Crack-tip loading from measured longitudinal residual stresses from welding process

Residual stresses in C(T) blank specimen

Keeping in mind the potential problems faced in the residual stress characterisation of such welds using neutron diffraction, because of the steep gradients over small length scale, it is necessary to have validated FE models to predict the J-integral and K_I, to assess the contribution of residual stresses towards fracture. In order to fulfil this requirement, two different FE models were developed as explained above. The reason to have two different models is to verify and validate the residual stresses in the C(T) blank specimen prior to crack introduction using two independent methods. The residual stress profile

across the weld at mid-thickness of the specimen predicted from both approaches are compared in Fig. 5. The longitudinal residual stress profile in the C(T) blank specimen from both specimen extraction simulation and residual stress mapping is shown in Fig. 5a and that of normal stress is shown in Fig. 5b. Observing the residual stress profiles, it can be concluded that the profiles match very well, indicating that the simulation has indeed predicted the residual stress distribution accurately. In all the subsequent analyses, the residual stresses were considered from the mapped model and the plastic strain history

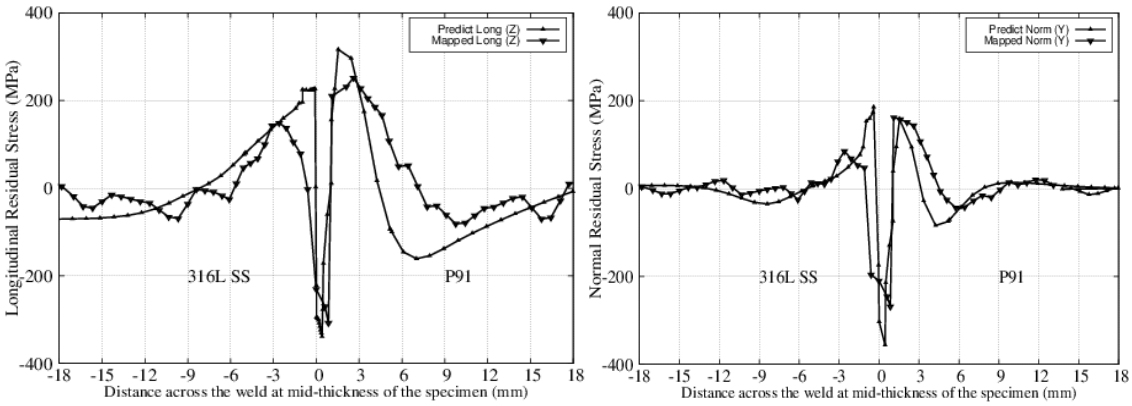

(a) (b)

Fig. 5. Comparison of (a) longitudinal and (b) normal residual stresses in C(T) blank from FE simulation and residual stress mapping methods.

Determination of modified J-Integral and K_I

To identify the influence of residual stresses from the welding process on the fracture behaviour of the material, several linear elastic and elastic-plastic loading cases were analysed using the validated C(T) blank specimen as described previously. Based on the numerical fracture analysis, the longitudinal residual stress field around the crack-tip is shown in Fig. 6. Comparing Fig. 6 with measured longitudinal residual profile around the crack-tip shown in Fig. 4, it is evident that the centre of the weld and thereby the crack-tip residual stress field is predominantly compressive. However, in Fig. 4, the tensile region adjacent to the compressive weld centre is approximately at a distance of 0.5 mm

whereas in Fig. 6, it is about 1 mm. Also, the magnitudes of the peak compressive and tensile stresses measured are different from the predictions. Despite these differences, a similarity in the trend is observed in both the contours.

The value of K_I is determined as -4.254 MPa√m using the weight function method. The predicted K_I due to crack-tip loading from secondary stresses is shown in Fig. 7. Given the lack of accurate material properties for the weld material and the corresponding uncertainties in the predicted residual stresses, the predicted value of -3.64 MPa√m is considered to be in reasonably good agreement with the value calculated using weight function approach.

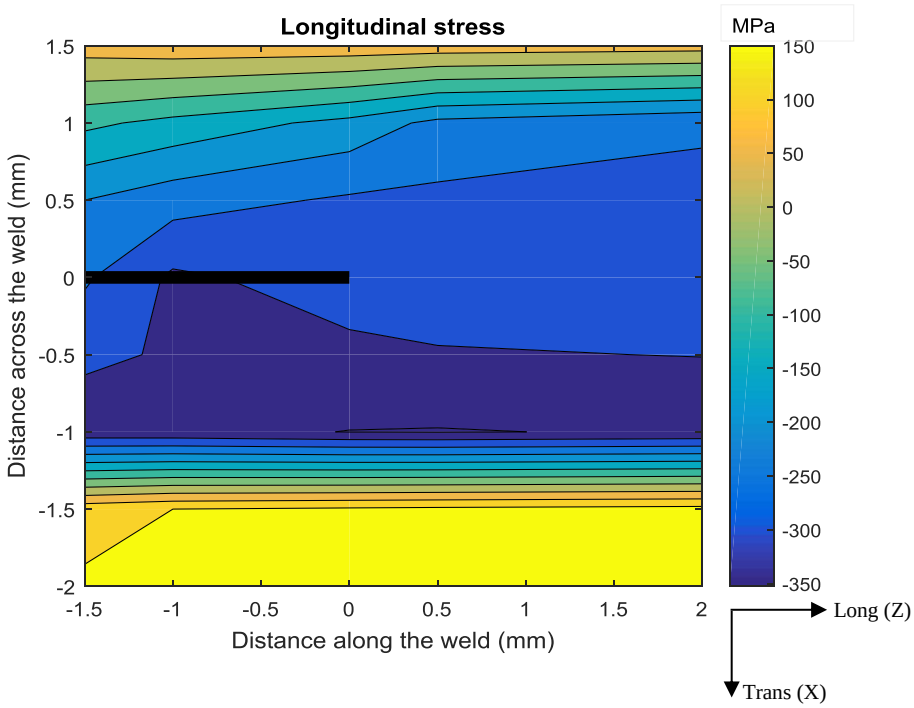

Fig. 6. Predicted longitudinal residual contour around the crack-tip

The variation of K_I with applied load with and without residual stress influence is shown in Fig. 8. The predicted values indicate strongly contour independent results even under combined primary and secondary loading. From the figure, it is apparent under linear elastic consideration, the stress-intensity factor from secondary loading linearly combines with that from the primary stresses. This value is independent of external load

and doesn't vary with it. Therefore, at relatively smaller loads, the contribution from the secondary stresses in the calculation of K_I is significant. Yet, as the primary loading increases, the contribution from primary load towards K_I rises drastically as opposed to that from residual stresses which is constant in comparison. Nevertheless, the effects of residual stresses exist even at higher loads and must be included in the fracture analysis. For the current material with compressive residual stress state ahead of the crack-tip, it is observed that K_I from combined loading is smaller than that of primary loading only.

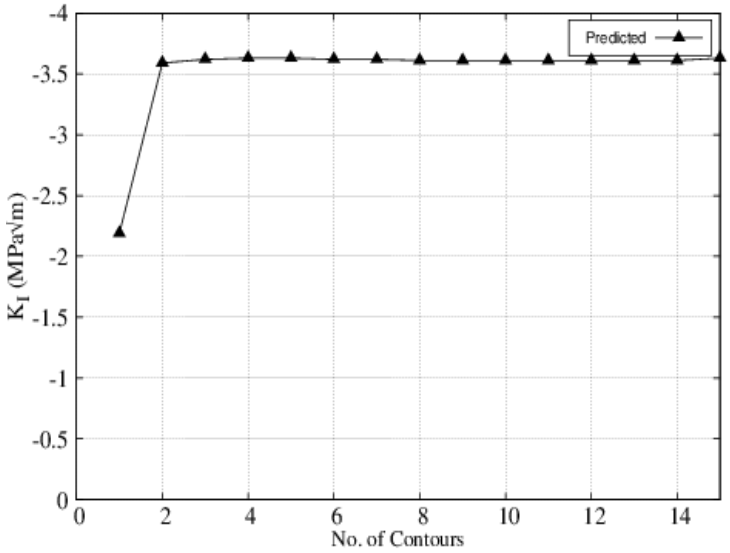

Fig. 7. Predicted K_I due to crack-tip loading from secondary stresses

The predicted modified J-integral using elastic-plastic analysis for secondary loading at mid-thickness of the C(T) specimen is shown in Fig. 9. The contour independence of the results is clearly evident from the graph.

As in the case of K_I from secondary stresses shown in Fig. 7, the predicted modified J-integral from secondary stresses is considerably small for this specimen. This implies that the crack transverse stress component is the main contributor in the evaluation of fracture parameters. For the current case, despite considerable amount of crack longitudinal and normal stresses (~ -300 MPa), the transverse stresses are relatively very small and therefore lead to small values of J-integral and K_I. The predicted modified

J-integral under combined primary and secondary loading for varying primary loads is shown in Fig. 10. The path independence of the contour results under all loading cases is notable in Fig. 10 (left).

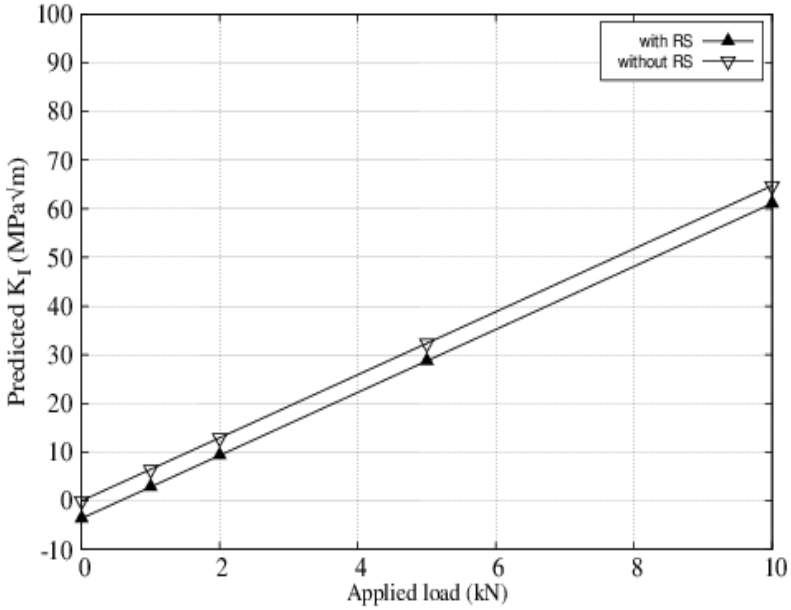

Fig. 8. Variation of predicted K_I with primary load and combined primary and secondary loading

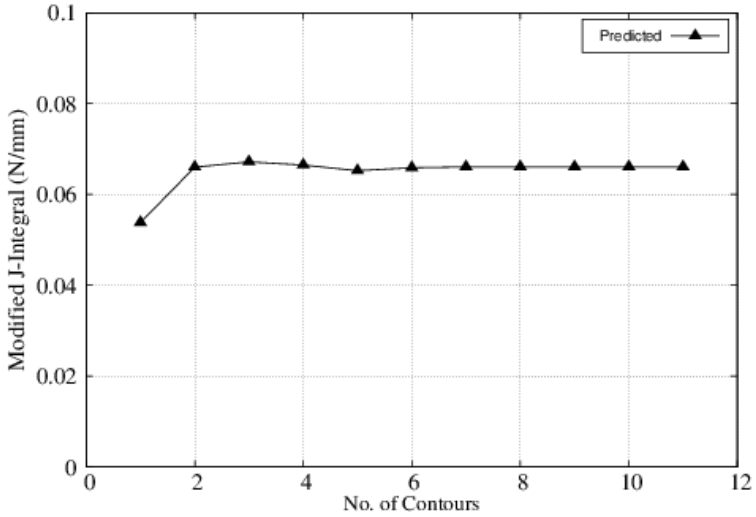

Fig. 9. Predicted modified J-integral values under secondary stresses only

It is observed that as the primary loading increases the difference in the predicted modified J-integral under primary stresses alone and that of combined stresses becomes more pronounced as depicted in Fig. 10 (right). A possible reason for this can be

explained through the individual contributions of initial plastic strain gradient associated with residual stresses towards evaluation of J-integral and the mechanical strain energy density from the residual stress field. For computing modified J-integral in Abaqus, the mechanical strain energy density from the initial residual stress field is calculated by removing the plastic strain energy density associated with initial residual stress field. This is constant with applied load whereas the effects of initial plastic gradient increase with increasing load. At lower primary loads, the residual stresses may contribute towards fracture. Nevertheless, under higher loads, these may be relaxed due to stress relaxation. However, the effects of plastic strain hardening exist even at higher loads indicating that

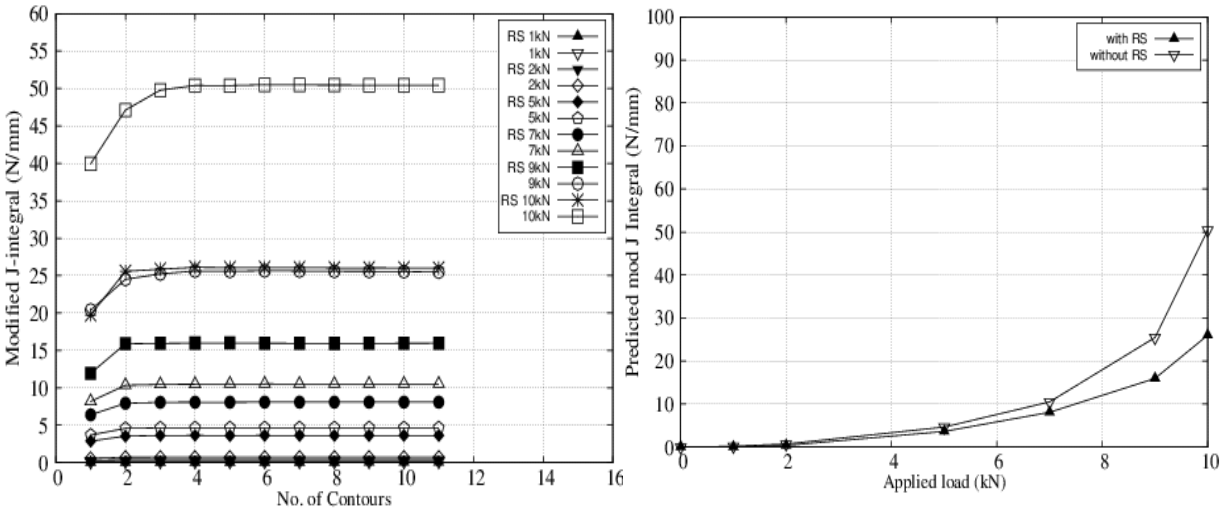

Fig. 10. Comparison of predicted modified J-integral for cases under primary loading only and combined primary and secondary loading

As experimental determination of J-integral is quite complicated and requires repetitive tests, often numerical simulation is a better alternative to estimate the fracture parameters and perform sensitivity studies, especially when there is limited supply of the raw material to be investigated. Owing to the experimental limitations in quantifying

initial plastic strains in a material from a manufacturing process, FE analysis offers a particular advantage in analysing cases with very high levels of prior plastic strain history such as welding process. However, such a prediction and sensitivity study is only valid when the simulation model is thoroughly validated.

Conclusions

Based on the experimental and numerical investigations performed for determining fracture parameters on a C(T) specimen extracted from a dissimilar weld made from P91 (ferritic/martensitic) steel and AISI 316LN stainless steel using autogenous EB welding, the following conclusions can be drawn:

1. The centre of the weld is predominantly under compression due to solid-state phase transformation (SSPT) experienced by P91 steel during welding cooling cycle. This is evidenced both in measurements as well as simulations indicating a very high compressive stress-state ahead of the crack-tip.
2. The relatively steep gradients in stress measured over a small length scale (~ 2mm) across the weld using neutron diffraction pose a significant complexity to analyse the crack behaviour in the interface region (weld and HAZ) in the presence of residual stresses, due to the extreme sensitivity of the results based on the location of the crack.
3. Numerical simulation offers a very good alternative to experimental investigation for fracture analysis of welds with steep stress gradients over a fine length scale, provided the model is sufficiently validated.
4. The effect of residual stresses on fracture under linear elastic conditions is constant irrespective of primary loading and resulted in reduced value of predicted K_I for the current material under consideration because of the compressive residual stresses ahead of the crack tip.

5. Under elastic-plastic analysis, the effects of residual stresses are felt from the initial plastic strain gradient associated with the residual stresses as well as the residual stress magnitude. The plastic strain history and residual stresses affect the predicted fracture parameter in a non-linear fashion. Although it is generally noticed that the effects of residual stresses wash out at higher primary stresses because of stress relaxation, the effects of prior plastic straining and the extent of initial plastic strains gradients have a considerable influence on fracture even at very high primary loads. Therefore, it is essential to carefully account for these in the analysis to predict accurate fracture behaviour under residual stresses.

Future work

The FE models developed for predicting the fracture behaviour of the dissimilar weld under combined primary and secondary loading will be validated through *in-situ* diffraction studies using neutron and synchrotron radiation. Using the validated models, the secondary stress relaxation under complex boundary conditions will be predicted accurately and advanced methods of structural integrity assessment, which take into account the relaxation of complex secondary stresses will be proposed using the modelling and prediction capability developed through this work.

Acknowledgement

We would like to acknowledge the support provided by IGCAR for the samples. This project was funded by an EPSRC project EP/K007866/1.

References

1. P.A. Eikrem, Z.L. Zhang, B. Nyhus. Effect of plastic prestrain on the crack tip constraint of pipelines. International Journal of Pressure Vessels and Piping 2007; 84:708 – 715.

2. Y. Lei, N.P.O'Dowd, G.A. Webster. Fracture mechanics analysis of a crack in a residual stress field. International Journal of Fracture 2000; 106:195 – 216.
3. R.A. Ainsworth, J.K. Sharples, S.D. Smith. Effects of residual stresses on fracture behaviour – experimental results and assessment methods. Journal of Strain Analysis 2000; 35(4): 307 – 316.
4. R6 – Assessment of the integrity of structures containing defects, Revision 4, EDF Energy Nuclear Generation Ltd.
5. BS 7910:2013 – Guide to methods for assessing the acceptability of flaws in metallic structures, BSI Standards Limited 2013.
6. R.A. Ainsworth. The treatment of thermal and residual stresses in fracture assessments. Engineering Fracture Mechanics 1986; 24(1): 65 – 76.
7. H-Y. Lee, F.R. Biglari, R. Wimpory, K.M. Nikbin. Treatment of residual stresses in failure assessment procedure. Engineering Fracture Mechanics 2006; 73: 1755 – 1771.
8. K. Abburi Venkata, C.E. Truman, D.J. Smith, Characterising residual stresses in a dissimilar metal electron beam welded plate. Procedia Engineering 2015; 130: 973 – 985.
9. K. Abburi Venkata, C.E. Truman, D.J. Smith, A.K. Bhaduri. Characterising electron beam welded dissimilar metal joints to study residual stress relaxation from specimen extraction. International Journal of Pressure Vessels and Piping 2016; 139-140: 237 – 249.
10. K. Abburi Venkata, C.E. Truman, D.J. Smith, R.C. Wimpory. Relaxation of residual stresses when extracting a specimen from a dissimilar metal electron beam welded plate. Proceedings of the 7th International Conference on Creep, Fatigue and Creep-Fatigue Interaction 2016.

11. K. Abburi Venkata, C.E. Truman, H.C. Coules, S. Khayatzadeh. Interaction of residual stresses with applied stresses in a dissimilar electron beam welded specimen. Proceedings of the 2016 International Conference on Pressure Vessels and Piping. 2016; V003T03A078-PVP2016-63494.
12. ASTM E1820 – 15a. Standard test method for measurement of fracture toughness. DOI:10.1520/E1820-15A.
13. M.T. Hutchings, P.J. Withers, T.M. Holden, T. Lorentzen. Introduction to the Characterization of Residual Stress by Neutron Diffraction. 2005. CRC Press, Taylor & Francis Group.
14. A. Lodini. Calculation of residual stress from measured strain. In: A. Lodini, M.E. Fitzpatrick. Analysis of Residual Stress by Diffraction Using Neutron and Synchrotron Radiation. Taylor & Francis. London and New York. 2003; 47–59.
15. Y. Lei. J Calculation for a crack in a welding residual stress field following a FE simulation. Transactions SMiRT-23. 2015.
16. X.R. Wu, A.J. Carlson. Weight function and stress intensity factor solutions. Pergamon Press, Oxford. England. 1991.